

Ionothermal Synthesis of Extra-Large-Pore Open-Framework Nickel Phosphite $5\text{H}_3\text{O}\cdot[\text{Ni}_8(\text{HPO}_3)_9\text{Cl}_3]\cdot 1.5\text{H}_2\text{O}$: Magnetic Anisotropy of the Antiferromagnetism**

Hongzhu Xing, Weiting Yang, Tan Su, Yi Li, Jin Xu, Takehito Nakano,* Jihong Yu,* and Ruren Xu

The chemistry of inorganic open-framework materials is one of the most active areas of chemical research because of their potential applications as absorbents, ion exchangers, and catalysts in heterogeneous catalysis.^[1] A challenging target in this field is the design and synthesis of extra-large microporous open frameworks so that catalysis and separation can be performed on large molecules.^[2] To achieve large pore openings, several approaches toward synthesis of materials with extra-large pores have been explored in the past few years.^[3] In particular, a number of interrupted open-framework phosphates with extra-large channels have been synthesized hydro-/solvolthermally in the presence of organic amines as structure-directing agents.^[4] Notably, replacement of tetrahedral phosphate groups PO_4^{3-} by pseudopyramidal phosphite units HPO_3^{2-} that can reduce the M-O-P connectivity would generate more-open interrupted frameworks. By using organic amines as structure-directing agents under hydro-/solvolthermal conditions, several metal phosphites with extra-large pore openings have been prepared by us and others. Notable examples are cobalt phosphite CoHPO-CJ2 ^[5] with 18-ring channels, ZnHPO-CJ1 ^[6] and Cr-NKU-24 ^[7] with extra-large 24-ring channels, and NTHU-5 ^[4d] with 26-ring channels.

Besides their traditional applications, microporous open-framework materials are finding new applications as advanced functional materials in optics, electronics, magnetism, and so on.^[8] Currently, the magnetic properties of porous

open frameworks are attracting much attention. Generation of open-framework materials that order magnetically is an important goal in materials chemistry. Pillaring of inorganic layers having high magneto-anisotropy is an important strategy for the generation of porous magnets. Notable examples are inorganic-organic hybrid 3D open frameworks originating from pillaring of inorganic metal hydroxides by amines or bicarboxylates, which show multiple magnetic properties.^[9] However, accounts on obtaining 3D inorganic open-framework magnets by pillaring lower-dimensional highly magneto-anisotropic systems are still rare.

Open-framework materials are typically synthesized by hydro-/solvolthermal methods. Ionothermal synthesis, that is, the use of an ionic liquid as solvent and sometimes structure-directing agent in the preparation of microporous crystalline solids, is currently receiving great attention because of the different chemistry of ionic-liquid solvent systems compared to the traditionally used water/alcohols in hydro-/solvolthermal synthesis.^[10] With the aim of exploring new porous materials with interesting magnetic properties, we report herein the first ionothermal synthesis of an open-framework nickel phosphite, namely, $5\text{H}_3\text{O}\cdot[\text{Ni}_8(\text{HPO}_3)_9\text{Cl}_3]\cdot 1.5\text{H}_2\text{O}$ (JIS-3) with extra-large 18-ring channels. We found that JIS-3 shows antiferromagnetic ordering, and investigated the magnetic anisotropy by measurements on aligned single crystals.

JIS-3 was prepared ionothermally from a mixture of the ionic liquid 3-methyl-1-pentylimidazolium hexafluorophosphate ($[\text{PMim}][\text{PF}_6]$), $\text{NiCl}_2\cdot 6\text{H}_2\text{O}$, and H_3PO_3 in a molar ratio of 10:1:2 at 130 °C. The phase purity was confirmed by the agreement between the experimental powder X-ray diffraction (XRD) pattern and the simulated pattern based on structure analysis (Figure S1, Supporting Information). The presence of Cl in the product was confirmed by X-ray photoelectron and energy-dispersive X-ray spectroscopic measurements (Figures S2 and S3, Supporting Information).

Single-crystal structural analysis revealed that the structure of the JIS-3 anionic framework consists of $[\text{Ni}_8(\text{HPO}_3)_9\text{Cl}_3]^{5-}$ units (Figure 1). Charge balance of the anionic framework is achieved by protonated water molecules located in channels. Each asymmetric unit contains two crystallographically distinct Ni sites and two crystallographically distinct P sites (Figure S4, Supporting Information). The Ni atoms are in a distorted octahedral environment: Ni(1) is coordinated to one $\mu\text{-O}$, one $\mu\text{-Cl}$, and four $\mu_3\text{-O}$ atoms forming Ni-O-P and Ni-O-Ni bonds; Ni(2), which lies on the threefold axis is coordinated to six $\mu_3\text{-O}$ atoms to form six

[*] H. Xing, W. Yang, T. Su, Dr. Y. Li, J. Xu, Prof. J. Yu, Prof. R. Xu
State Key Laboratory of Inorganic Synthesis
and Preparative Chemistry
College of Chemistry, Jilin University
Changchun 130012 (P. R. China)
Fax: (+86) 431-8516-8608
E-mail: jihong@jlu.edu.cn
Prof. T. Nakano
Department of Physics, Graduate School of Science
Osaka University, Toyonaka, Osaka 560-0043 (Japan)
E-mail: nakano@nano.phys.sci.osaka-u.ac.jp

[**] We thank the National Natural Science Foundation of China, the State Basic Research Project of China (grants 2006CB806103 and 2007CB936402), and the Major International Collaboration Project of China for financial support for this work. T.N. acknowledges a Grant-in-Aid for Scientific Research on Priority Areas (No. 19051009) and a Grant-in-Aid for Young Scientists B (no. 20710077) from MEXT (Japan).

Supporting information for this article is available on the WWW under <http://dx.doi.org/10.1002/ange.200906471>.

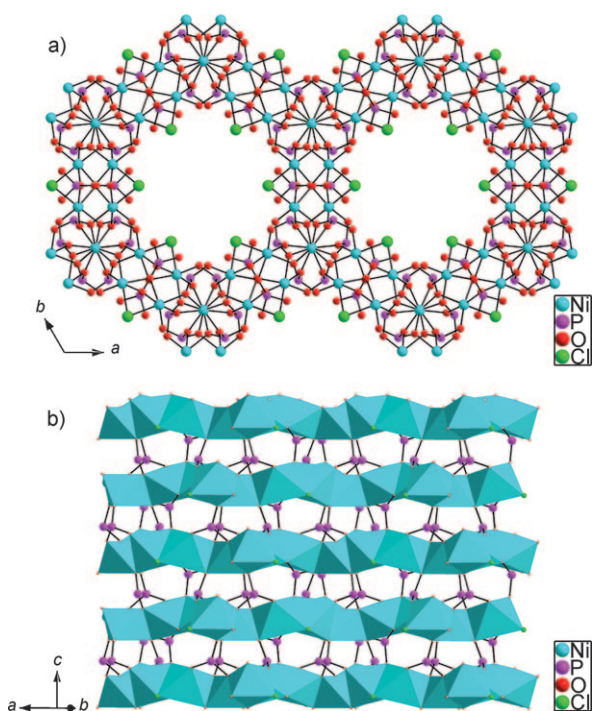


Figure 1. a) The framework of JIS-3 viewed along the [001] direction showing 18-ring channels. b) A view showing that the 2D nickel–oxygen/chloride layers stacked along the *c* axis are pillared by HPO₃ units to form the 3D open-framework structure.

Ni–O–P bonds. The Ni–O bond lengths vary in the range of 2.016(5)–2.116(5) Å, and the Ni–Cl bond length is 2.453(3) Å. Bond valence sum (BVS) calculations show that both Ni(1) and Ni(2) have the oxidation state of +2. The P(1) atom connects two μ_3 -O and one μ -O atom to Ni(1) and Ni(2), leaving a terminal P–H bond. The P(2) atom, located on the mirror plane, connects two Ni(1) atoms through two μ_3 -O atoms, leaving two terminal sites occupied by O and H atoms, respectively. Oxygen atom O(2) is disordered over two crystallographically equivalent sites, and the resulting P(2)=O(2) bond length is 1.508(10) Å. The P–O_{bridging} bond lengths (av 1.517 Å) are in agreement with those observed in other metal phosphites. The existence of the P–H bond is confirmed by the characteristic bands of phosphite anions [$\tilde{\nu}(\text{H–P}) = 2468$ and 2418 cm^{−1}] in the IR spectrum (Figure S5, Supporting Information).

The structure of JIS-3 is built up by connection of Ni(1)O₅Cl octahedra, Ni(2)O₆ octahedra, and HPO₃ pseudopyramids to give a 3D open framework with extra-large 18-ring channels along the [001] direction (Figure 1a). Interestingly, its structure features a 2D nickel–oxygen/chloride 18-ring layer (Figure S6a, Supporting Information) composed of alternating dimers of face-sharing Ni(1)-centered octahedra and edge-sharing Ni(2)-centered octahedra. Each Ni(2)O₆ octahedron lying on the threefold axis shares edges with three adjacent Ni(1)O₅Cl octahedra to form a windmill unit (Figure S6b, Supporting Information). These windmill units are connected to each other by face sharing between neighboring Ni(1)O₅Cl octahedra, which results in an infinite 2D layered structure with 18-ring windows. Such

18-ring 2D layers are stacked along the *c* axis in an AB sequence, where layers A and B are related by a 6_3 screw axis. The size of the 18-ring window is approximately 11 Å. The layers stacked along the *c* axis are further linked by HPO₃ pseudopyramids to form the 3D open-framework structure (Figure 1b) of JIS-3. An XRD study showed that JIS-3 is thermally stable up to 300°C with release of the water molecules of crystallization. Further loss of the protonated water molecules above 300°C results in the collapse of the framework.

The dc magnetic susceptibility (χ_m) of JIS-3 was measured on a polycrystalline sample at 5 kOe in the 4–300 K range (Figure S7, Supporting Information). The magnetic susceptibility data above 50 K are fitted very well by the Curie–Weiss law [$\chi_m = C/(T - \theta)$], which gives a Curie constant of 1.25 cm³ K mol^{−1} and a Weiss temperature of +14.2 K. The $\chi_m T$ value increases with decreasing temperature and reaches a maximum at 8 K, decreases quickly as the temperature drops further, and finally reaches a value of 0.75 cm³ K mol^{−1} at 4 K (Figure 2a). This behavior indicates a predominant

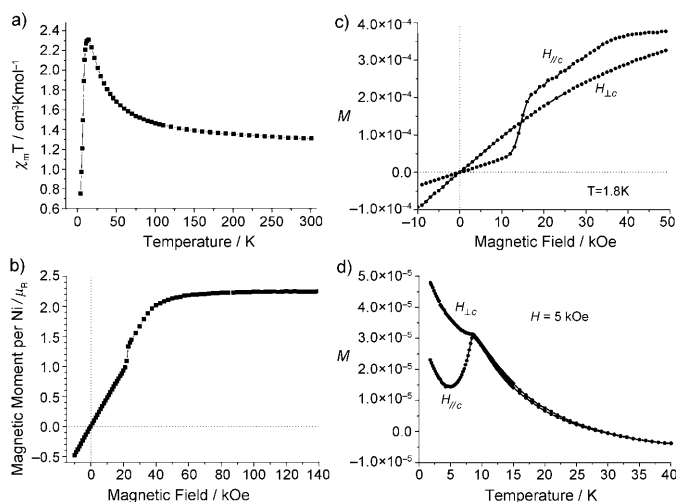


Figure 2. $\chi_m T$ versus *T* (a) and magnetization curve (b) of JIS-3 for a powder sample. Magnetization *M* curve (c) and temperature-dependent magnetization (d) of JIS-3 on aligned single-crystal samples under applied fields of $H_{||c}$ and $H_{\perp c}$ (raw data).

ferromagnetic (FM) interaction in the material at high temperatures and finally antiferromagnetic (AFM) interaction in the low-temperature region. The positive Weiss temperature further confirms the dominant FM interactions in the high-temperature region. The maximum of χ_m observed at 8.5 K (Figure S7, Supporting Information) suggests long-range AFM ordering in the low-temperature region.

To further investigate the underlying magnetic nature, measurements of ac magnetic susceptibility were carried out at a field of $H_{dc} = 0$, $H_{ac} = 2$ Oe in the range 2–30 K (Figure S8, Supporting Information). The real part (χ') of the ac susceptibility shows a detectable maximum at 8.5 K, which fits well with $T_N = 8.5$ K observed from the χ_m curve. Moreover, no peak in the imaginary part (χ'') was observed. The ac magnetic susceptibility further confirms that JIS-3 shows AFM interaction at low temperature.

Figure 2b shows the magnetization curve for a polycrystalline powder sample at magnetic fields up to $H = 14$ T (140 kOe) at 1.8 K. The saturation magnetization obtained from this data is $2.25 \mu_B$ per Ni ion. This is consistent with the $S = 1$ state of Ni^{2+} ions, because typically the Ni^{2+} ion has a Landé g factor of about 2.2, and a magnetic moment of $2.2 \mu_B$ is expected. Hence, it is clear that the AFM ground state is realized by localized magnetic moments of Ni^{2+} ions. At around 20 kOe in the magnetization curve, it shows a spin-flop-like behavior characteristic of antiferromagnets.^[11] The spin flop is related to the magnetic anisotropy and it is rather difficult to discuss only on the basis of the data on the polycrystalline sample. Hence, we carried out magnetization measurements on “single”-crystal samples up to $H = 5$ T (50 kOe). For single crystal measurements, we picked out more than ten nice crystals and aligned them on Scotch tape in the same direction under a microscope. A bundle of crystals was fixed to the sample holder to avoid reorientation of the crystals, which would occur whenever the sample is moved or oscillates during the measurement. Therefore, the difference between $H_{\parallel c}$ and $H_{\perp c}$ data comes only from the magnetic anisotropy effect. Figure 2c shows the magnetization curve under the applied field of $H_{\parallel c}$ and $H_{\perp c}$ at 1.8 K. Due to the very small mass of the crystals, the absolute values of the magnetization can not be obtained. The units here are arbitrary although they stay constant between measurements. The spin-flop behavior is observed only under $H_{\parallel c}$. From these data it can be concluded that the easy axis of the antiferromagnetic state is the c axis, that is, the magnetic moments are oriented to the direction of the c axis at zero field due to the magnetic anisotropy. Under $H_{\perp c}$, it is hard to saturate the magnetization, as is seen in the high-field region. This is also an effect of the magnetic anisotropy.

Figure 2d shows the temperature dependence of the single-crystal magnetization under an applied field of 5 kOe. A peak at near the Néel temperature of 8.7 K is clearly observed under $H_{\parallel c}$, but not so clearly under $H_{\perp c}$. This is also consistent with the easy axis being the c axis in this sample. The negative values of the magnetization in the high-temperature region ($T > 30$ K) may result from the unsubtracted diamagnetic component of the sample and the Scotch tape. In conclusion, nickel phosphite JIS-3 is in an AFM ground state with Ni^{2+} ($S = 1$) localized magnetic moments and the c direction as easy axis.

Considering the crystal structure, the intralayer interaction is due to Ni-O-Ni super-exchange coupling, and the interlayer interaction to Ni-O-P-O-Ni super-exchange coupling. The magnetic exchange interactions in near-neighbor Ni-O-Ni coupling should be stronger than the Ni-O-P-O-Ni coupling. As mentioned above, the FM interaction is dominant in JIS-3 due to the positive Weiss temperature as well as the shape of the $\chi_m T$ versus T curve. Therefore, the stronger intralayer coupling through the Ni-O-Ni bonding should be FM. It is, however, clear that the magnetic ground state is AFM. Thus, the weaker interlayer coupling through the Ni-O-P-O-Ni bonding should be AFM, which leads to the AFM long-range order at low temperature. These assumptions are consistent with theoretical predictions on the super-exchange mechanism,^[12] which state that the 90° bonding angle between

Ni^{2+} ions gives FM superexchange coupling, while the 180° bonding angle results in AFM coupling. The Ni-O-Ni bond angles in the layer range between 88 and 100° and are thus close to 90° and result in FM superexchange coupling. Consequently, the following magnetic structure of JIS-3 can be proposed with high probability: 1) The intralayer near-neighbor Ni-O-Ni superexchange coupling (FM) is much stronger than the interlayer Ni-O-P-O-Ni superexchange coupling (AFM). 2) The spins in layers A and A', which are related by inversion symmetry and stacked along the c axis in the structure, are oppositely oriented, and the magnetic moments are oriented to the easy c axis.

In summary, we have presented the ionothermal synthesis of an open-framework metal phosphite by using an ionic liquid as solvent. The new compound has extra-large 18-ring channels in the framework. Its structure features 2D nickel-oxygen/chloride 18-ring layers composed of alternating face-sharing dimers of Ni(1)-centered octahedra and edge-sharing Ni(2)-centered octahedra. These layers are further pillared by pseudopyramidal HPO_3 groups to form the 3D open framework. Magnetic measurements show that JIS-3 orders antiferromagnetically with spin-flop transition at a befitting applied field. Measurements on aligned single crystals indicate that the spins in the 2D nickel-oxygen/chloride 18-ring layers are oppositely oriented, and the magnetic moments are oriented to the easy c axis. The successful preparation of nickel phosphite JIS-3 in an ionic liquid demonstrates not only that the ionothermal method is a promising method to synthesize novel open-framework materials with extra-large pore openings, but also that pillaring of inorganic layers having high magneto-anisotropy is a feasible strategy for generating 3D porous magnets.

Experimental Section

The details of the ionothermal synthesis and characterization of JIS-3 are provided in the Supporting Information.

Crystal data for JIS-3: $0.88 H_3O \cdot [Ni_{1.33}(HPO_3)_{1.5}Cl_{0.5}] \cdot 0.25 H_2O$, $M_r = 231.83$, space group $P6_3cm$ (No. 185), $a = 14.871(2)$, $c = 9.2822(19)$ Å, $V = 1777.8(5)$ Å³, $Z = 12$, 1443 unique reflections out of 16627 with $I > 2\sigma(I)$, $3.16 > \theta > 27.46^\circ$, 87 parameters, final R factors $R_1 = 0.0431$ [$I > 2\sigma(I)$] and $wR_2 = 0.1118$ (all data), GOF = 1.06. Further details on the crystal structure investigations may be obtained from the Fachinformationszentrum Karlsruhe, 76344 Eggenstein-Leopoldshafen, Germany (fax: (+49) 7247-808-666; e-mail: crysdata@fz-karlsruhe.de), on quoting the depository number CSD-421123.

Received: November 17, 2009

Published online: February 28, 2010

Keywords: ionothermal synthesis · layered compounds · magnetic properties · microporous materials · nickel

- [1] a) A. Corma, H. Garcia, *Chem. Rev.* **2003**, *103*, 4307–4365; b) J. Yu, R. Xu, *Chem. Soc. Rev.* **2006**, *35*, 593–604.
- [2] a) M. E. Davis, *Nature* **2002**, *417*, 813–814; b) M. E. Davis, C. Saldarriaga, C. Montes, J. Garces, C. Crowder, *Nature* **1988**, *331*, 698–699.

- [3] a) Y.-L. Lai, K.-H. Lii, S.-L. Wang, *J. Am. Chem. Soc.* **2007**, *129*, 5350–5351; b) J. Sun, C. Bonneau, Á. Cantín, A. Corma, M. J. Díaz-Cabañas, M. Moliner, D. Zhang, M. Li, X. Zou, *Nature* **2009**, *458*, 1154–1157; c) X. Ren, Y. Li, Q. Pan, J. Yu, R. Xu, Y. Xu, *J. Am. Chem. Soc.* **2009**, *131*, 14128–14129.
- [4] a) Q. Huo, R. Xu, S. Li, Z. Ma, J. M. Thomas, R. H. Jones, A. M. Chippindale, *J. Chem. Soc. Chem. Commun.* **1992**, 875–876; b) N. Guillou, Q. Gao, M. Nogues, R. E. Morris, M. Hervieu, G. Férey, A. K. Cheetham, *C. R. Acad. Sci. Ser. IIc* **1999**, *2*, 387–392; c) G. Yang, S. C. Sevov, *J. Am. Chem. Soc.* **1999**, *121*, 8389–8390; d) C. H. Lin, S. L. Wang, K. H. Lii, *J. Am. Chem. Soc.* **2001**, *123*, 4649–4650.
- [5] L. Zhao, J. Li, P. Chen, G. Li, J. Yu, R. Xu, *Chem. Mater.* **2008**, *20*, 17–19.
- [6] J. Liang, J. Li, J. Yu, P. Chen, Q. Fang, F. Sun, R. Xu, *Angew. Chem.* **2006**, *118*, 2608–2610; *Angew. Chem. Int. Ed.* **2006**, *45*, 2546–2548.
- [7] Y. Yang, N. Li, H. Song, H. Wang, W. Chen, S. Xiang, *Chem. Mater.* **2007**, *19*, 1889–1891.
- [8] a) Y. C. Liao, C. H. Lin, S. L. Wang, *J. Am. Chem. Soc.* **2005**, *127*, 9986–9987; b) A. Shulman, A. E. C. Palmqvist, *Angew. Chem.* **2007**, *119*, 732–736; *Angew. Chem. Int. Ed.* **2007**, *46*, 718–722; c) Q. Gao, N. Guillou, M. Nogues, A. K. Cheetham, G. Férey, *Chem. Mater.* **1999**, *11*, 2937–2947.
- [9] a) M. Kurmoo, H. Kumagai, S. M. Hughes, C. J. Kepert, *Inorg. Chem.* **2003**, *42*, 6709–6722; b) A. Rujiwatra, C. J. Kepert, J. B. Claridge, M. J. Rosseinsky, H. Kumagai, M. Kurmoo, *J. Am. Chem. Soc.* **2001**, *123*, 10584–10594; c) M. Kurmoo, *Chem. Mater.* **1999**, *11*, 3370–3378; d) M. Kurmoo, *J. Mater. Chem.* **1999**, *9*, 2595–2598.
- [10] a) E. R. Cooper, C. D. Andrews, P. S. Wheatley, P. B. Webb, P. Wormald, R. E. Morris, *Nature* **2004**, *430*, 1012–1016; b) E. R. Parnham, R. E. Morris, *Acc. Chem. Res.* **2007**, *40*, 1005–1013; c) Z. Ma, J. Yu, S. Dai, *Adv. Mater.* **2010**, *22*, 261–285.
- [11] a) S. Foner, *Phys. Rev.* **1963**, *130*, 183–197; b) L. J. de Jongh, W. D. van Amstel, A. R. Miedema, *Physica* **1972**, *58*, 277–304.
- [12] J. Kanamori, *J. Phys. Chem. Solids* **1958**, *10*, 87–98.